DOI: 10.1002/chem.200801266

Ground Spin State Changes and 3D Networks of Exchange Coupled [Mn^{III}_3] Single-Molecule Magnets

Ross Inglis,[b] Leigh F. Jones,[b] Kevin Mason,[b] Anna Collins,[b] Stephen A. Moggach,[b] Simon Parsons,[b] Spyros P. Perlepes,[c] Wolfgang Wernsdorfer,*[a] and Euan K. Brechin*[b]

The field of single-molecule magnetism began in the early 1990s with the discovery that a discrete dodecametallic Mn cluster exhibited hysteresis in magnetisation versus field studies.[1–3] The potential of using molecules for such applications as information storage and quantum computing thus propelled the synthesis and characterisation of many more molecules displaying similar properties.[3] A fascinating example within this family is the manganese cluster $[Mn_4O_3Cl_4(O_2CEt)_3(py)_3]$ which crystallises as a supramolecular H-bonded dimer of $[\{Mn_4\}_2]$ cubanes.[4,5] Antiferromagnetic coupling between the two components results in quantum behaviour different from that of the individual single-molecule magnets (SMMs), suggesting a means of tuning the quantum tunnelling of magnetisation (QTM) in SMMs and indicating that exchange-coupled SMMs in one, two and three dimensions may display fascinating physical properties.[6–8]

We recently reported the synthesis and magnetic properties of a large family of hexanuclear Mn^{III} SMMs based on the complex $[Mn^{III}_6O_2(sao)_6(O_2CH)_2(EtOH)_4]$ ($saoH_2$ = salicylaldoxime).[9–12] We showed that, by using derivatised versions of the oxime ligand (R–sao^{2-} R = H, Me, Et etc), it was possible to significantly increase the ground spin state from $S = 4$ to $S = 12$, greatly enhancing the effective energy barrier for magnetisation reversal.[9–11] The origin of the antiferromagnetic (AF)→ferromagnetic (F) switch arises from a structural distortion of the molecule, induced by the "twisting" of the (-Mn-N-O-) ring, as evidenced by the significant increases in the Mn-N-O-Mn torsion angles when bulkier salicylaldoximes are employed.[12] The ability to deliberately switch pairwise exchange interactions in such a controllable fashion has enormous potential, but understanding in detail the underlying contributory factors in such complicated molecules is an extremely difficult task, as it is the consequence of a number of different super-exchange pathways. To further elucidate these factors and to examine whether the same effect can be seen in different molecules we have synthesised analogous "half" $[Mn_6]$ molecules, that is, the species $[Mn^{III}_3O(R–sao)_3(O_2CR)(solvent)_{3,4}]$ (R = H, Me, Et, Ph etc.) in which we systematically increase the puckering of the molecules through targeted structural distortions of the oxime moiety.

After an extensive synthetic study we have discovered a number of routes to these $[Mn^{III}_3O(R–sao)_3(O_2CR)(solvent)_{3,4}]$ triangles (Figure 1 shows complexes **1** and **5**). These include using various combinations of pyridine as solvent or co-solvent and bulky carboxylic acids and oximes (for example, Ph–$saoH_2$; see the Supporting Information for full experimental details). Pyridine molecules cap one face of the triangle preventing dimerisation to the hexametallic unit. For example, the reaction of $Mn(O_2CMe)_2{\cdot}4H_2O$ with Me–$saoH_2$ in pyridine affords $[Mn^{III}_3O(Me–sao)_3(OAc)(py)_4]{\cdot}2py$ (**1**·2py). The core of **1** (Figure 1a) comprises the common $\{Mn^{III}_3O\}^{7+}$ oxo-centred triangle whose edges are bridged in a $\eta^1{:}\eta^1{:}\eta^1{:}\mu$-fashion by the doubly deprotonated Me-sao^{2-} ligands, to form three Mn-N-O-Mn pathways between the metal ions. The $\eta^1{:}\eta^1{:}\mu$-bridging ^-O_2CMe ligand straddles the "top" of the $\{Mn^{III}_3O(Me–sao)_3\}^+$ moiety bonding to two Mn^{III} centres (Mn1 and Mn2). The remaining site on the upper face is occupied by a

[a] Prof. W. Wernsdorfer
Institut Néel
CNRS & Université J. Fourier, BP 166
38042 Grenoble (France)
Fax: (+33) 476881191
E-mail: wolfgang.wernsdorfer@grenoble.cnrs.fr

[b] R. Inglis, Dr. L. F. Jones, K. Mason, Dr. A. Collins, Dr. S. A. Moggach, Prof. S. Parsons, Dr. E. K. Brechin
School of Chemistry
The University of Edinburgh
West Mains Road, Edinburgh, EH9 3JJ (UK)
Fax: (+44) 1316506453
E-mail: ebrechin@staffmail.ed.ac.uk

[c] Prof. S. P. Perlepes
Department of Chemistry
University of Patras
26504 Patras (Greece)

Supporting information for this article is available on the WWW under http://dx.doi.org/10.1002/chem.200801266.

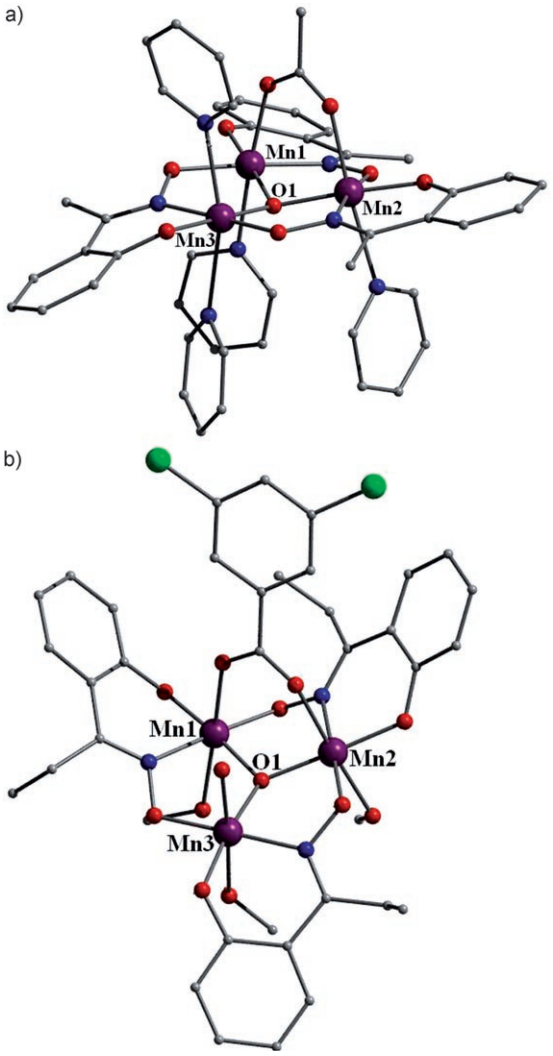

Figure 1. The molecular structure of complexes **1** (a) and **5** (b). Colour code: Mn purple, O red, N blue, C grey, Cl green.

pyridine molecule, as are all three axial sites at the base of the molecule, completing the distorted octahedral coordination geometry at each Mn^{III} centre; the Jahn–Teller axes being perpendicular to the $[Mn_3]$ plane. The effect of the pyridine molecules and the relatively small oxime is the generation of a relatively flat (or nonpuckered) $\{Mn^{III}{}_3O(Me\text{-}sao)_3\}^+$ moiety with Mn-N-O-Mn torsion angles in the range 4.15–23.44° (Table 1). Replacement of ^-O_2CMe and Me–sao^{2-} with a) $^-O_2CPh(Me)_4$ and sao^{2-} and b) ^-O_2C–anthra (HO_2C–anthra = anthracene-9-carboxylic acid) and Me–sao^{2-} (in py/EtOH) produces the analogous complexes $[Mn^{III}{}_3O(sao)_3(O_2CPh(Me)_4)(py)_3]\cdot EtOH$ (**2**·EtOH) and $(pyH\cdot Na)[Mn^{III}{}_3O(Me\text{–}sao)_3(O_2C\text{–}anthra)(py)_3]_2(ClO_4)_2\cdot py$ (**3**·py), respectively. The only differences to **1** being that one site on the upper face remains unoccupied (Mn3 is five-coordinate), presumably owing to the presence of the much bulkier carboxylate. In **3**, a six-coordinate Na^+ ion connects two symmetry-equivalent $\{Mn^{III}{}_3O(Me\text{-}sao)_3(O_2C\text{–}anthra)(py)_3\}$ moieties together forming a [{Mn_3}-Na-{Mn_3}] dimer (Na–O bond lengths range: 2.310–2.680 Å, Figure SI1 in the Supporting Information). The charge is balanced by two symmetry-equivalent ClO_4^- counterions and one pyridinium cation, which is H-bonded to the pyridine solvent molecule.

In the absence of pyridine, the hexametallic complexes $[Mn^{III}{}_6O_2(R\text{-}sao)_6(O_2CR)_2(EtOH)_4(H_2O)_2]$ form.[12] This complexation can be avoided by using a combination of a bulky oxime and a bulky carboxylate. For example, the reaction between $Mn^{II}(ClO_4)\cdot 6H_2O$, Et–$saoH_2$ and either $NaO_2CPh(CF_3)_2$ or $NaO_2CPh(Cl)_2$ in ROH forms the complexes $[Mn^{III}{}_3O(Et\text{–}sao)_3(O_2Ph(CF_3)_2)(EtOH)(H_2O)_3]\cdot EtOH\cdot 3H_2O$ (**4**·EtOH·3 H_2O; Figure SI2 in the Supporting Information) and $[Mn^{III}{}_3O(Et\text{–}sao)_3(O_2CPh(Cl)_2)(MeOH)_3(H_2O)]$ (**5**), respectively; and the reaction of $Mn^{II}(ClO_4)\cdot 6H_2O$, Ph–$saoH_2$ and NaO_2C–anthra in MeOH produces $[Mn^{III}{}_3O(Ph\text{–}sao)_3(O_2C\text{–}anthra)(MeOH)_4]\cdot Ph\text{–}saoH_2$ (**6**·Ph–$saoH_2$; Figure SI2–SI4 in the Supporting Information). The core structures of **4–6** are again simple oxo-centred triangles similar to **1–3**, differing only in the identity of the terminally bound solvent molecules, the presence/absence of counterions and co-crystallised organic molecules. The major structural changes are a dramatic increase in the Mn-N-O-Mn torsion angles (Table 1), which can be attributed to the presence of bulkier R–$saoH_2$ ligands (R = Me- (**1, 3**), H- (**2**) Et- (**4, 5**), Ph- (**6**). The result is an increasingly puckered $\{Mn^{III}{}_3O(R\text{-}sao)_3\}$ unit, albeit with the central Mn-O-Mn angles remaining relatively undistorted, ranging from a minimum of 113.57(5)° to a maximum of 118.00(5)° in **1** and from 110.80(10) to 121.54(8)° in complexes **2–6** (Table 1). In each case the central μ_3-O^{2-} ion is raised above the $\{Mn_3\}$ plane by a minimum of 0.178 Å in **6** to a maxi-

Table 1. Magneto-structural parameters for complexes **1-6**.

	Torsion angles [°]			Mn-O-Mn [°]			Mn_3 plane–μ_3 dist(sd) [Å]O	J [cm^{-1}]	S	g	U_{eff} [K]
	Mn(1–2)	Mn(2–3)	Mn(1–3)	Mn1-O1-Mn2	Mn2-O1-Mn3	Mn1-O1-Mn3		$J_1/J_2/J_3$			
1	4.15	4.45	23.44	113.57(5)	117.89(5)	118.00(5)	0.359	−1.58, −0.10	2	2.07	–
2[a]	24.38	5.33	11.06	112.70(2)	118.20(2)	117.10(2)	0.383	–	2	–	–
	31.99	11.06	3.04	112.80(2)	116.30(2)	119.00(2)	0.382				
3	16.35	11.74	26.58	110.80(10)	114.86(10)	116.99(11)	0.464	−1.20, −1.94, −0.40	2	2.02	–
4	46.66	38.56	40.35	115.83(13)	119.96(14)	119.84(14)	0.179	+1.52	6	1.98	43
5	44.6	38.17	39.07	115.33(7)	120.10(7)	118.71(7)	0.265	+1.84	6	2.02	51
6	32.98	34.41	41.44	115.80(8)	121.54(8)	119.98(8)	0.178	+0.85, +1.44	6	1.98	–

[a] Complex **2** contains two independent $[Mn^{III}{}_3]$ units in the asymmetric unit and thus no attempt to fit the data was made.

mum of 0.464 Å in **3** (Table 1). Previous studies on analogous [Mn_6] molecules suggest that such an increase in the torsion angles should lead to a switch in the exchange between the metal ions from antiferromagnetic to ferromagnetic.[12] In each case there are significant H-bonding interactions and close intermolecular contacts propagated in all three dimensions (see Figure SI1–4 in the Supporting Information), which has important consequences for the magnetic behaviour.

Direct current (dc) magnetisation measurements were carried out on polycrystalline samples of **1–6** in a field of 0.1 T and a temperature range of 5–300 K. These are plotted in Figure 2. Room-temperature magnetic susceptibility ($\chi_m T$)

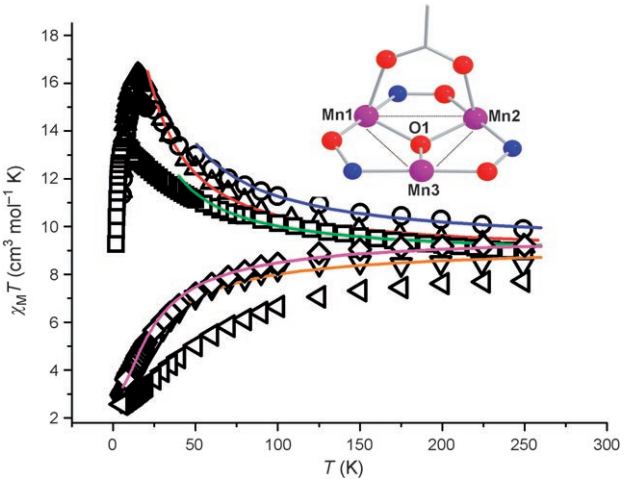

Figure 2. Plot of χ_MT versus T for complexes **1–6**. The solid lines represent the best fits of the data. See text for details. Inset: magnetic coupling scheme employed. **1** ◇, **2** ◁, **3** ▽, **4** △, **5** ○, **6** □.

values for **1–6** range from 8.42 to 9.90 $cm^3 mol^{-1} K$ and are consistent with the expected value for three non-interacting Mn^{III} centres (~9.0 $cm^3 mol^{-1} K$). Compounds **1–3** exhibit a dominant antiferromagnetic exchange between the Mn^{III} ions, with the values of $\chi_m T$ remaining relatively constant as the temperature is decreased before dropping more sharply at approximately 125 K, to values of 3.61, 2.57 and 2.72 $cm^3 mol^{-1} K$ at 5 K, respectively. A fit of the experimental data using the 2 J model (J_1 (that mediated through oxide, oxime and carboxylate) $\neq J_2 = J_3$ (that mediated through oxide and oxime), Figure 2 (inset)) of Equation (1) afforded the parameters $S=2$, $g=2.07$, $J_1=-1.58$, $J_2=-0.10$ cm^{-1} for **1** (Table 1), but proved unsuccessful for **3**, which required the 3 J model ($J_1 \neq J_2 \neq J_3$) of Equation (1), giving $S=2$, $g=2.02$, $J_1=-1.2$, $J_2=-1.94$ and $J_3=-0.4$ cm^{-1} (Table 1).

$$\hat{\mathscr{H}} = -2J_1[(\hat{S}_1 \cdot \hat{S}_2)] - 2J_2[(\hat{S}_2 \cdot \hat{S}_3)] - 2J_3[(\hat{S}_1 \cdot \hat{S}_3)] \quad (1)$$

No attempt was made to fit the data for **2**, as the crystal structure contains two independent molecules with different geometries (Table 1). The plots of $\chi_m T$ versus T for complexes **4–6** (Figure 2) indicate the presence of ferromagnetic exchange between the Mn^{III} centres. In each case $\chi_m T$ rises gradually as the temperature is decreased before increasing more rapidly at lower temperatures and peaking at values of 16.36 (complex **4**), 15.30 (complex **5**) and 13.34 $cm^3 mol^{-1} K$ (complex **6**) , respectively (Figure 2). A sharp drop in $\chi_m T$ then occurs in all three cases, presumably as a result of the intermolecular interactions and/or zero-field splitting effects; the low temperature maxima being significantly lower than the value of 21.0 $cm^3 mol^{-1} K$ expected for $S=6$. Fitting of the data obtained for **4** and **5** using the 1 J spin-Hamiltonian ($J_1=J_2=J_3$) described in Equation (1), affords the parameters $S=6$, $g=1.98$, $J=+1.52$ cm^{-1} and $S=6$, $g=2.02$, $J=+1.84$ cm^{-1}, respectively. A similar model was unsuccessful for **6**, and required the 2 J model ($J_1 \neq J_2 = J_3$) of Equation (1), giving $S=6$, $g=1.98$, $J_1=+0.85$ and $J_2=+1.44$ cm^{-1}.

The structural and magnetic information summarised in Table 1 allows us to make some conclusions with respect to the origin of the ferromagnetism in salicylaldoxime-based [Mn^{III}_3O]$^{7+}$ complexes: a) There appears to be little or no correlation between the exchange and the distance between the [Mn_3] plane and the O^{2-} ion. Previous studies on similar systems have suggested an increasingly ferromagnetic interaction as this distance increases;[13a] a trend not shown here. b) There appears to be little or no correlation between the exchange and the Mn-O-Mn bridging angle. Experimental studies of [$Mn^{III}_3O(O_2CR)_6L_3$]$^+$ species suggest a switch from antiferromagnetic to ferromagnetic at angles below approximately 120°[14]— a phenomenon not detected here. c) There is little or no correlation between the Mn^{III}–O^{2-} distance and the exchange, since all six complexes display similar values ranging from a minimum of 1.868(3) Å to a maximum of 1.919(2) Å. d) There appears to be little or no correlation between the exchange and the Mn–N–O–Mn bond lengths. e) There appears to be a correlation between the exchange and the Mn-N-O-Mn torsion angle: the larger the torsion angle, the more ferromagnetic the pairwise exchange, as previously reported for the "parent" [Mn_6] complexes,[12] and suggested by recent DFT calculations,[13b] which allows us to conclude that while all of the above interactions must play some role in determining the sign and magnitude of J, it appears the dominant factor is the twisting of the Mn-N-O-Mn moiety.

Alternating current (ac) susceptibility studies were carried out on crystalline samples of **4–6** in the temperature range 1.8–10.0 K in a 3.5 G field oscillating at frequencies between 50 and 1000 Hz. Frequency-dependent out-of-phase (χ_M'') signals (Figure 3), suggestive of SMM behaviour, were detected for complexes **4–6** with peaks at temperatures of 3.8 and 3.4 K at 300 Hz for **4** and **5** respectively, whereas only the tails of peaks were observed for **6**. These data were then used to construct Arrhenius plots, from which fitting of the Arrhenius equation gave $U_{eff} \approx 43$ K, $\tau_0 = 7.4 \times 10^{-9}$ s for **4**, and $U_{eff} \approx 51$ K, $\tau_0 = 1.2 \times 10^{-10}$ s for **5**. These are amongst the largest effective barriers known for low nuclearity SMMs. Hysteresis loop and relaxation measurements were carried

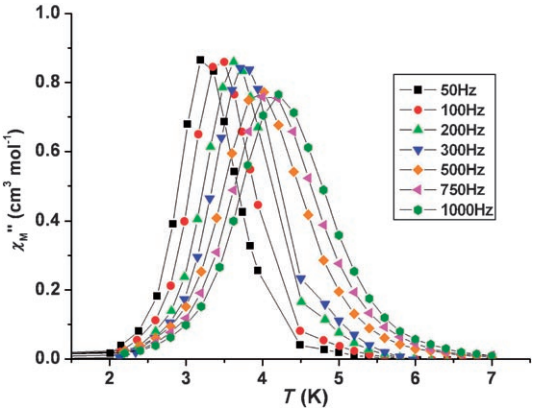

Figure 3. Plot of the out-of-phase (χ''_M) ac susceptibility versus temperature for **4** at the indicated frequencies.

out on single crystals of **4–6** using a micro-SQUID assembly, with the field applied along the easy axis of magnetisation.[15] In each case temperature- and sweep-rate-dependent hysteresis loops were observed, confirming SMM behaviour for all three complexes. Those obtained for **4** are shown in Figure 4. The loops display step-like features separated by plateaus. After saturating the magnetisation, the first resonance is seen in negative fields, indicating the presence of small intermolecular antiferromagnetic interactions, as was first established for [{Mn_4}$_2$].[4] Small modifications of the ligands surrounding this dimer led to three-dimensional networks of exchange-coupled SMMs.[16] A detailed study of the hysteresis loops of **4** show that the collective spins of each [Mn_3] molecule are coupled antiferromagnetically to its neighbouring molecules, acting as a bias that shifts the quantum tunnelling resonances with respect to the isolated SMM. Most of the small steps are therefore due to molecules having one or several "reversed" neighbouring molecules; although some of the steps may also be due to multibody quantum effects.[17] These findings are supported on examination of the crystal structure of **4**, which exhibits extensive intermolecular H-bonding interactions (Figure 4b, full description in the Supporting Information). The complexity of the system makes it extremely difficult to determine all of the active exchange pathways and to identify the steps. However, the field separation between two resonances yields a typical exchange bias field between two molecules of approximately 0.14 T. The field separation between the first and second biggest steps for fast field-sweep rates can be estimated as $D = 1.6$ K, leading to a barrier of $DS^2 =$ 58 K, where D = axial zero-field splitting parameter and DS^2 = upper limit to magnetisation reversal, somewhat larger than the effective barrier from the ac data. The above result suggests that a three-dimensional network of exchange-coupled SMMs does not suppress QTM. The intermolecular interactions are strong enough to cause a clear field bias, but too weak to transform the spin network into a classical antiferromagnet. This three-dimensional network of exchange coupled SMMs demonstrates that QTM can be controlled using exchange interactions, opening up new per-

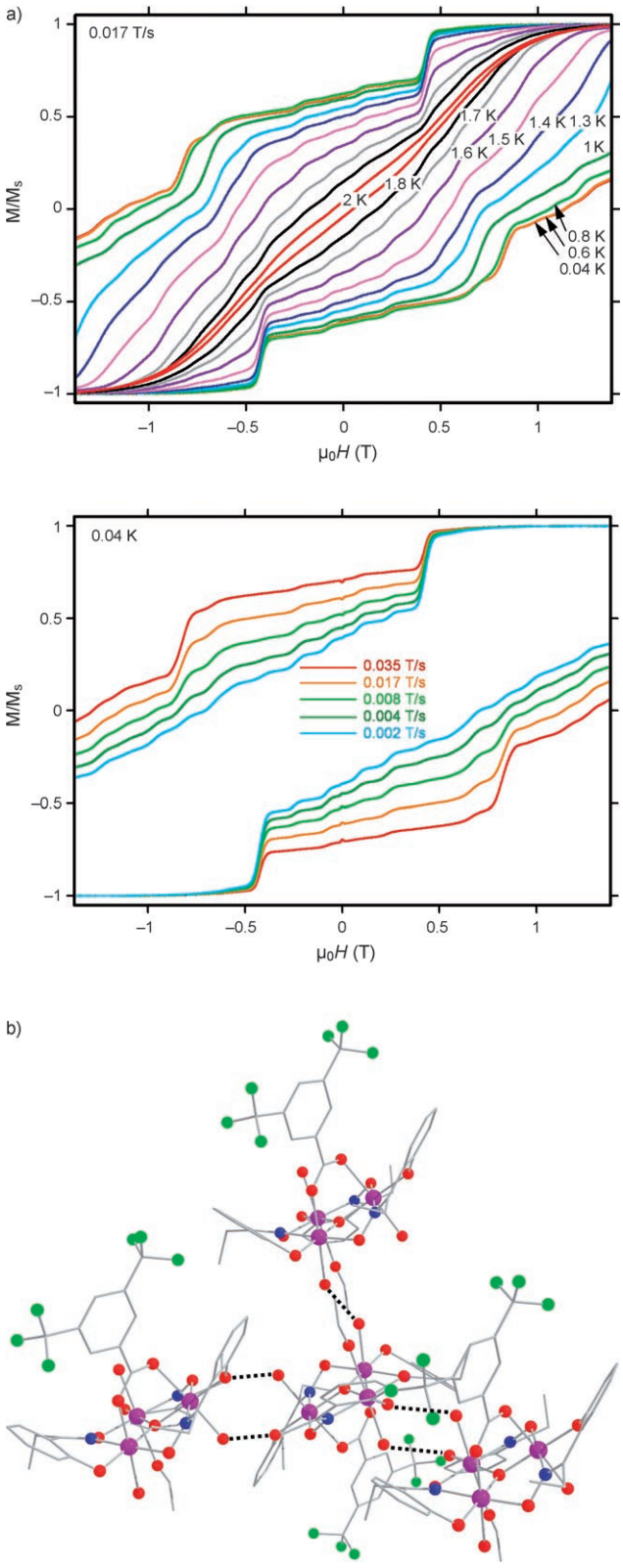

Figure 4. a) Magnetisation versus field hysteresis loops for a single crystal of **4** at the indicated temperatures and field sweep rates. M is normalised to its saturation value. b) The H-bonding between clusters of **4** in the crystal, propagated in the main via the oxime O atoms interacting with the terminal H_2O protons and -CF_3 groups. For full details see the Supporting Information. Colour code: Mn purple, O red, N blue, C grey, F green.

spectives in the use of supramolecular chemistry to modulate the quantum physics of molecular nanomagnets.

Experimental Section

Full experimental and crystallographic details for **1**–**6** are given in the Supporting Information. CCDC-628200 (**1**), CCDC-667573 (**2**), CCDC-667574 (**3**), CCDC-667575 (**4**), CCDC-667576 (**5**) and CCDC-667577 (**6**) contain the supplementary crystallographic data for this paper. These data can be obtained free of charge from The Cambridge Crystallographic Data Centre via www.ccdc.cam.ac.uk/data_request/cif.

Acknowledgements

The authors acknowledge The Leverhulme Trust for financial support.

Keywords: hysteresis · magnetic properties · manganese · oximes · structural distortion

[1] D. Gatteschi, R. Sessoli, *Angew. Chem.* **2003**, *115*, 278–309; *Angew. Chem. Int. Ed.* **2003**, *42*, 268–297.
[2] D. Gatteschi, R. Sessoli, J. Villain, *Molecular Nanomagnets*, Oxford University Press, Oxford, **2006**, and references therein.
[3] Single-Molecule Magnets and Related Phenomena (Ed.: R. E. P. Winpenny), *Struct. Bonding*, **2006**, *122*, 1–262 and references therein.
[4] W. Wernsdorfer, N. Aliaga-Alcalde, D. N. Hendrickson, G. Christou, *Nature* **2002**, *416*, 406–409.
[5] S. Hill, R. S. Edwards, N. Aliaga-Alcalde, G. Christou, *Science* **2003**, *302*, 1015–1018.
[6] C. Boskovic, R. Bircher, P. L. W. Tregenna-Piggott, H. U. Güdel, C. Paulsen, W. Wernsdorfer, A.-L. Barra, E. Khatsko, A. Neels, H. Stoeckli-Evans, *J. Am. Chem. Soc.* **2003**, *125*, 14046–14058.
[7] J. Yoo, W. Wernsdorfer, E.-C. Yang, M. Nakano, A. L. Rheingold, D. N. Hendrickson, *Inorg. Chem.* **2005**, *44*, 3377–3379.
[8] a) H. Miyasaka, M. Yamashita, *Dalton Trans.* **2007**, 399–404; b) H. Miyasaka, K. Nakata, L. Lecren, C. Coulon, Y. Nakazawa, T. Fujisaki, K. Sugiura, M. Yamashita, R. Clérac, *J. Am. Chem. Soc.* **2006**, *128*, 3770–3783.
[9] C. J. Milios, A. Vinslava, P. A. Wood, S. Parsons, W. Wernsdorfer, G. Christou, S. P. Perlepes, E. K. Brechin, *J. Am. Chem. Soc.* **2007**, *129*, 8–9.
[10] C. J. Milios, A. Vinslava, S. Moggach, S. Parsons, W. Wernsdorfer, G. Christou, S. P. Perlepes, E. K. Brechin, *J. Am. Chem. Soc.* **2007**, *129*, 2754–2755.
[11] C. J. Milios, A. Vinslava, W. Wernsdorfer, A. Prescimone, P. A. Wood, S. Parsons, S. P. Perlepes, G. Christou and E. K. Brechin, *J. Am. Chem. Soc.* **2007**, *129*, 6547–6561.
[12] C. J. Milios, R. Inglis, A. Vinslava, R. Bagai, W. Wernsdorfer, S. Parsons, S. P. Perlepes, G. Christou, E. K. Brechin, *J. Am. Chem. Soc.* **2007**, *129*, 12505–12511.
[13] a) T. C. Stamatatos, D. Foguet-Albiol, S.-C. Lee, C. C. Stoumpos, C. P. Raptopoulou, A. Terzis, W. Wernsdorfer, S. Hill, S. P. Perlepes, G. Christou, *J. Am. Chem. Soc.* **2007**, *129*, 9484–9499, and references therein; b) J. Cano, T. Cauchy, E. Ruiz, C. J. Milios, T. T. Stamatatos, S. P. Perlepes, G. Christou, E. K. Brechin. *Dalton Trans.* **2008**, 234–240.
[14] a) J. B. Vincent, H. R. Chang, K. Folting, J. C. Huffman, G. Christou, D. N. Hendrickson, *J. Am. Chem. Soc.* **1987**, *109*, 5703–5711; b) R. D. Cannon, R. P. White, *Prog. Inorg. Chem.* **1988**, *36*, 195–298.
[15] W. Wernsdorfer, *Adv. Chem. Phys.* **2001**, *118*, 99–190.
[16] R. Tiron, W. Wernsdorfer, N. Aliaga-Alcalde, G. Christou, *Phys. Rev. B* **2003**, *68*, 140407.
[17] a) W. Wernsdorfer, S. Bhaduri, R. Tiron, D. N. Hendrickson, G. Christou, *Phys. Rev. Lett.* **2002**, *89*, 19720; b) W. Wernsdorfer, S. Bhaduri, A. Vinslava, G. Christou, *Phys. Rev. B* **2005**, *72*, 214429.

Received: June 25, 2008
Published online: September 3, 2008

